OPEN ACCESS

University of BRISTOL

Link to published version (if available):
10.1021/acs.jcim.9b00918

Link to publication record in Explore Bristol Research
PDF-document

University of Bristol - Explore Bristol Research
General rights

Discovery of New and Potent InhA Inhibitors as Anti-tuberculosis Agents: Structure Based Virtual Screening Validated by Biological Assays and X-ray Crystallography

Pharit Kamsri,[1] Chayanin Hanwarinroj,[2] Naruedon Phusi,[2] Thimpika Pornprom,[2] Kampanart Chayajarus,[2] Auradee Punkvang,[1] Nitima Suttipanta,[3] Potjanee Srimanote,[4] Khomson Suttisintong,[5] Chomphunuch Songsiriritthigul,[6] Patchreenart Saparpakorn,[7] Supa Hannongbua,[7] Siriluk Rattanabunyong,[8] Supaporn Seetaha,[8] Kiattawee Choowongkomon,[8] Sanya Sureram,[9] Prasat Kittakoop,[9,10,11] Poonpilas Hongmanee,[12] Pitak Santanirand,[12] Zhaoqiang Chen,[13] Weiliang Zhu,[13] Rosemary A. Blood,[14] Yuiko Takebayashi,[14] Philip Hinchliffe,[14] Adrian J. Mulholland,[15] James Spencer,[14] and Pornpan Pungpo[2,*]

[1] Division of Chemistry, Faculty of Science, Nakhon Phanom University, 48000 Nakhon Phanom, Thailand

[2] Department of Chemistry, Faculty of Science, Ubon Ratchathani University, Warinchamrap, 34190 Ubonratchathani, Thailand

[3] Faculty of Pharmaceutical Sciences, Ubon Ratchathani University, Warinchamrap, 34190 Ubonratchathani, Thailand

[4] Faculty of Allied Health Sciences, Thammasat University, Rangsit Campus, 12120 Pathumthani, Thailand

[5] National Nanotechnology Center, National Science and Technology Development Agency, Thailand Science Park, 12120 Pathumthani, Thailand

[6] Synchrotron Light Research Institute (Public Organization), 30000 Nakhon Ratchasima, Thailand

[7] Department of Chemistry, Faculty of Science, Kasetsart University, Chatuchak, 10900 Bangkok, Thailand

[8] Department of Biochemistry, Faculty of Science, Kasetsart University, 10900 Bangkok, Thailand

9 Chulabhorn Research Institute, 10210 Bangkok, Thailand

10 Chulabhorn Graduate Institute, Chemical Biology Program, Chulabhorn Royal Academy,

10210 Bangkok, Thailand

11 Center of Excellence on Environmental Health and Toxicology (EHT), CHE, Ministry of Education, Bangkok, Thailand

12 Division of Microbiology, Department of Pathology, Faculty of Medicine, Ramathibodi Hospital, Mahidol University, 10400 Bangkok, Thailand

13 State Key Laboratory of Drug Research, Drug Discovery and Design Center, Shanghai Institute of Materia Medica, 201203 Shanghai, China

14 School of Cellular and Molecular Medicine, University of Bristol, Biomedical Sciences Building, University Walk, BS8 1TD Bristol, United Kingdom

15 Centre for Computational Chemistry, School of Chemistry, University of Bristol,

BS8 1TS Bristol, United Kingdom

E-mail: pornpan_ubu@yahoo.com

Abstract: The enoyl-acyl carrier protein reductase InhA of *M. tuberculosis* is an attractive, validated target for anti-tuberculosis drug development. Moreover, direct inhibitors of InhA remain effective against InhA variants with mutations associated with isoniazid resistance, offering the potential for activity against MDR isolates. Here, structure based virtual screening supported by biological assays was applied to identify novel InhA inhibitors as potential anti-tuberculosis agents. High-speed Glide SP docking was initially performed against two conformations of InhA differing in the orientation of the active site Tyr158. The resulting hits were filtered for drug-likeness based on Lipinski's rule and avoidance of PAINS-like properties, and finally subjected to Glide XP docking to improve accuracy. Sixteen compounds were identified and selected for in vitro biological assays, of which two (compounds **1** and **7**) showed MIC of 12.5 and 25 µg/ml against *M. tuberculosis* H37Rv, respectively. Inhibition assays against purified recombinant InhA determined IC_{50} values for these compounds of 0.38 and 0.22 µM,

respectively. A crystal structure of the most potent compound, compound **7**, bound to InhA revealed the inhibitor to occupy a hydrophobic pocket implicated in binding the aliphatic portions of InhA substrates but distant from the NADH cofactor, i.e. in a site distinct from those occupied by the great majority of known InhA inhibitors. This compound provides an attractive starting template for ligand optimization aimed at discovery of new and effective compounds against *M. tuberculosis* that act by targeting InhA.

Keywords: Tuberculosis, InhA, Virtual screening, Biological assays, X-ray crystallography

Introduction

Tuberculosis (TB) caused by *Mycobacterium tuberculosis* (*M. tuberculosis*) remains a major worldwide public health problem, especially in areas of high population density and low and middle-income countries. It is the leading cause of death by infectious disease and the ninth leading overall cause of death worldwide. World Health Organization (WHO) data identified 1.6 million TB deaths and 10 million new TB cases in 2017.[1] Although TB is considered treatable, this is threatened by the spread of drug resistant strains; it is estimated that globally there are 4.9 million cases of patients infected with multidrug-resistant tuberculosis (MDR-TB) strains resistant to isoniazid and rifampicin, the two most important anti-TB agents. In 2017 558,000 new cases of TB were identified that were resistant to rifampicin (RR-TB), the most effective first-line drug, with 82% of these MDR-TB. About 8% of TB patients worldwide are estimated to be infected with rifampicin susceptible, isoniazid-resistant strains (HR-TB).[2]

The *M. tuberculosis* enoyl-acyl carrier protein (ACP) reductase (*M. tuberculosis* InhA) is an attractive potential target for development of new anti-tuberculosis drugs. InhA catalyzes the NADH-specific reduction of 2-*trans*-enoyl-ACP (Figure 1A) in the elongation cycle of the fatty acid synthase type II (FAS II) pathway, the final step of fatty acid biosynthesis in *M. tuberculosis*.[3-4] InhA is the primary target of isoniazid (INH), the second first-line drug for tuberculosis treatment.[5-7] However, the inhibitory activity of isoniazid is reduced by mutations either in InhA or, more commonly, in the KatG catalase-peroxidase responsible for converting the INH prodrug into its active form.[8-10] Thus, identifying inhibitors that directly bind to InhA without the requirement for activation by KatG (direct InhA inhibitors) may represent a valid

strategy to overcome isoniazid resistance.[11-12] Hence multiple academic and pharmaceutical efforts have led to discovery of direct InhA inhibitors.[13-18] However, most of the direct InhA inhibitors so far identified display good InhA inhibitory activity in vitro, but poor activity against *M. tuberculosis*.[13,19-21]

The interactions of InhA with substrate, cofactor and inhibitors have been extensively studied.[22] One outcome of these investigations is the identification of the active site residue Tyr158 as important both to stabilizing the substrate during the catalytic reaction of *M. tuberculosis* InhA and to the binding of direct InhA inhibitors.[3-4, 23] Two different conformations of the Tyr158 sidechain have been identified in binding of direct InhA inhibitors (Figure 1B), an "in" conformation associated with the ternary InhA complex (substrate/cofactor-bound form), and an "out" conformation resembling that observed in the binary InhA complex (cofactor-bound form).[19-24]

In the present work, we have applied structure based virtual screening to select candidate InhA inhibitors from the compound library of the Specs database (www.specs.net), seeking to account for the mobility of Tyr158 by including both conformations of this residue in the screening workflow. This protocol identified two compounds that showed both inhibitory activity against *M. tuberculosis* cell growth and sub-micromolar inhibition of purified InhA in in vitro activity assays. A crystal structure for the complex of the most potent of these with InhA identified inhibitor binding in a hydrophobic active site pocket utilized in substrate binding and with Tyr158 in the "in" conformation. These findings demonstrate that these approaches can identify compounds with InhA inhibitory activity that are active against *M. tuberculosis*.
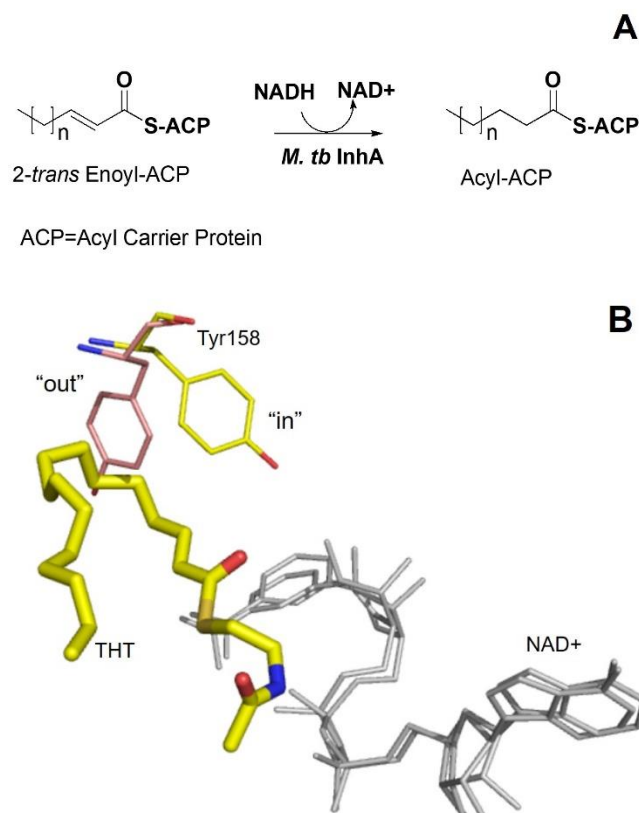
Figure 1. NADH-specific reduction of 2-*trans*-enoyl-ACP catalyzed by InhA (A), in and out conformations of Tyr158 sidechain (B). Tyr158 in the "in" conformation (yellow) in the ternary InhA structure complexed with the C16 substrate analogue THT (*trans*-2-hexadecenoyl-(*N*-acetylcysteamine)-thioester (yellow carbon atom) and NAD^{+} (gray) and Tyr158 in the "out" conformation (pink) in the binary InhA structure complexed with NAD^{+} (gray). PDB codes of these structures are 1BVR[3] and 1ENY[6], respectively.

Materials and Methods

Structure based virtual screening approach

Structure based virtual screening was employed to search the novel InhA inhibitors from a ligand library of Specs database (Figure 2). Initially, all small molecules (~200,000 compounds) contained in Specs database were docked to InhA-inTyr158 and InhA-outTyr158 receptors using Glide program[25-27] with the standard precision (SP) mode, to reduce the time-consuming. Then, top 2,000 compounds ranked by Glide SP score obtained from each receptor were selected for

further step. This is followed by the selection of compounds that showed good Glide SP scores for binding in both InhA-inTyr158 and InhA-outTyr158. Subsequently, the selection of Lipinski's rule of five[28-29] and pan-assay interference compounds (PAINS)[30] were employed as the drug-likeness filter. Then, all filtered compounds were docked to both InhA-inTyr158 and InhA-outTyr158 by using the extra precision (XP) mode that showed higher accuracy than the SP mode. Top compounds that show good Glide scoring function obtained from XP Glide docking (Glide XP score) in both InhA-inTyr158 and InhA-outTyr158 receptors were selected as the hit compound. All hit compounds were subjected for biological assays.

Molecular docking calculations

Molecular docking calculations were performed by the Glide program.[25-27] InhA with the "in" and "out" conformations of Tyr158 (InhA-inTyr158 and InhA-outTyr158, respectively) were considered as receptors for virtual screening. InhA complexed with a diphenyl ether derivative (PT70) (PDB code: 2X23)[20] and that complexed with a *N*-((3*R*,5*S*)-1-(benzofuran-3-carbonyl)-5-(ethylcarbamoyl)pyrrolidin-3-yl)-3-ethyl-1-methyl-1*H*-pyrazole-5-carboxamide (KV1) (PDB code: 4COD)[21] were selected as the representative InhA-inTyr158 and InhA-outTyr158, respectively. The Protein Preparation Wizard Workflow integrated in the Maestro was employed to prepare receptor with PROPKA at pH 7.0 for amino acid protonation assignment. Then, receptors with OPLS-2005 force field were minimized with the heavy atoms restrained (RMSD of 0.3 Å). Small compounds were prepared with LigPrep module provided in the Maestro program. The protonation states of compounds were generated with Epik at pH of 7.0 ± 2.0. Grid box was set by the default protocol and centered by the ligand.

Plasmid expression for *M. tuberculosis* H37Rv InhA

To facilitate the expression of InhA enzyme, the InhA gene was amplified by forward primer 5'AT<u>CATATG</u>ACAGGACTGGACGGC 3' and reverse primer 5'ACGCCG<u>GATCC</u>TAGAGCATTTGG 3'which introduced the 5' *NdeI* restriction site and 3' *BamHI*. restriction site. The slowdown PCR was used to amplify an 810 bp InhA amplicon. The amplicon was digested with *NdeI* and *BamHI* and cloned to pET15b. The InhA-pET15b plasmid that contained hexa-histidine at *N*-terminal (InhA-6xHis enzyme) was transformed into *E. coli* BL21(DE3) for enzyme expression

Overexpression and purification of InhA enzyme

Culture of BL21(DE3) cell carrying the wild type InhA was grown in 5 L of LB ampicillin (100 µg/mL) medium at 37°C to an OD_{600} of 0.6, and subsequently induced with 50 µM isopropyl-β-D-thiogalactopyranoside (IPTG). After shaking at 250 rpm for 4 hr. at 29°C, the bacterial cell was harvested by centrifugation at 4,000 rpm for 10 min at 4°C. The bacterial pellet was resuspended in 20 mM Tris-HCl, pH 7.9, containing 500 mM NaCl. The bacterial cell was lysed by French press at 2,000 psi and followed by centrifuging at 14,000 rpm for 30 min at 4°C to remove cell debris. The supernatant was applied to Ni-NTA chromatography and InhA was eluted by using a gradient of 250 mM imidazole. The fraction contain InhA were pooled and exchanged into 30 mM pierazine-1,4-bis (2-ethanesulfonic acid) (PIPES) buffer pH 6.8, containing 150 mM NaCl and 1 mM EDTA via PD-10 desalting columns equilibrated with PIPES 30 mM pH 6.8, 150 mM NaCl to remove imidazole. The elution fractions from desalting column were pooled and concentrated with Vivaspin centrifugal concentrator. Nanodrop was used to determine the concentration and SDS-PAGE was used to analyze the purity of InhA. For protein crystallization, InhA was thrombin cleaved to remove the *N*-terminal His-tag prior to buffer exchange into 30 mM PIPES pH 6.8, 150 mM NaCl using a PD-10 desalting column.

Relative inhibition of InhA inhibitors

Triclosan, NADH and DMSO were obtained from Sigma-Aldrich. Inhibitors were collected from the Specs database (www.specs.net). Stock solutions of the inhibitors were prepared in DMSO such that the final concentration of this co-solvent was constant at 1% (v/v) in the final volume of 100 µL for all kinetic reactions. The relative inhibition for InhA of selected compounds was evaluated in 200 µL of 30 mM PIPES buffer, pH 6.8 containing 1 mg/ml BSA, 50 µM NADH, 75 µM *trans*-2-dodecenoyl-CoA (DD-CoA) and 1 µM InhA inhibitor. The plate was shaken for 1 min and finally the reactions were initiated by adding InhA at 15 nM final concentration. The mixer of InhA and NADH was preincubated at 25 °C for 5 min followed by the addition of compound and continually preincubated at 25 °C for 20 min. The reactions were started by adding 75 µM DD-CoA. The reaction was run for 10 min at 25 °C following the fluorescence intensity of NADH at excitation λ = 340 nm and emission λ = 420 nm. The fluorescence intensity of NADH of each well was recorded every 30 seconds. The relative inhibitory activ1ity

of each compound was expressed as % relative inhibition of InhA (initial velocity of the reaction) with respect to control reaction without the inhibitor as calculated in equation 1.

$$\% \ relative \ inhibition = 100 \times \left(\frac{F_{compound} - F_{negative \ control}}{F_{positive \ control} - F_{negative \ control}} \right) \qquad (1)$$

$F_{compound}$ is the fluorescence intensity of the enzymatic activity for each compound concentration. $F_{positive}$ control is the fluorescence intensity of the enzyme activity in the absence of any compound, and $F_{negative}$ control is the fluorescence intensity of the NADH oxidation in the absence of the enzyme. Positive control wells contained DMSO. Negative control wells did not contain InhA enzyme. Triclosan was used to be the positive control. For those sample showing at least 60% inhibition, the follow up verification conducted in triple-triplicate in the IC_{50} determination mode.

IC_{50} Determination

Briefly, IC_{50} values were also determined in 96-well plates with the serial 3-fold dilution with assay buffer that contained DMSO of each inhibitor. The final condition of DMSO in the final assay was 1%. The IC_{50} value was determined by at least 8 concentrations, with each triple-triplicate under saturation condition. The relative inhibition of InhA was calculated as described above. IC_{50} values were calculated from plots of enzyme activity versus the log of inhibitor concentration.

Anti-mycobacterial assay

Microplate Alamar blue assay (MABA) was used to determine the minimum inhibitory concentration (MIC) against *M. tuberculosis* of hit compounds. Hit compounds were dissolved in DMSO (Sigma), and subsequently diluted two-fold in 100 mL of Middlebrook 7H9GC in the 96-well plate. A mycobacterial suspension was prepared in 0.04% Tween 80 and diluted with sterile distilled water to a turbidity of the McFarland no. 1. The suspension was then diluted 1:50 with 7H9GC, and 100 mL of this suspension was added to wells of microplates. After incubation at 37 °C for approximately 7 days, 12.5 mL of 20% Tween 80 and 20 mL of Alamar blue (SeroTec Ltd, Oxford, UK) were added to all wells. Growth of the organisms was determined after pre-

incubation at 37 °C for 16-24 h by visual determination of a colour change from blue to pink. The MIC is defined as the lowest concentration that prevents the colour change. Triclosan (Sigma) was used as a standard drug. Clinical isolates of *M. tuberculosis* were obtained from a stock culture of Ramathibodi Hospital, Bangkok, Thailand, and they were obtained during routine diagnostic work (most cultures collected during 2000-2005). The ethics committee of Ramathibodi Hospital has approved the use of these clinical isolates for this study.

Crystallization, data collection and structure solution

InhA crystals were grown under similar conditions as previously described[24, 31] using sitting-drop vapor diffusion in 24 well plates (Hampton Research). Drops containing 1.5 µl protein (13 mg/ml) and 1 µl reservoir solution (17% w/v PEG 4000, 0.1 M ADA pH 6.8, 6 mM DMSO, 0.1 M ammonium acetate, 1% glycerol, 4.5 mM NAD$^+$) were equilibrated against 500 µl of reservoir solution. Trays were incubated at 19 °C and crystals grew to their maximum size within 3-5 days. InhA complexed with compound **7** was obtained by soaking crystals overnight in 10 mM compound , 25% glycerol v/v, 17% w/v PEG 4000, 0.1 M ADA pH 6.8, 6 mM DMSO, 0.1 M ammonium acetate, 1% glycerol, 4.5 mM NAD$^+$ at 4°C. X-ray data were collected at 100 K on beamline I03 (Diamond Light Source, United Kingdom), integrated using XDS[32] in the Xia2[33] pipeline and scaled using Aimless[34] in the CCP4 suite[35]. Crystallographic phases were solved using Phaser[36] with PDB 4BQP[24] as the starting model, and 6 molecules in the asymmetric unit. Early rounds of refinement were completed in Refmac5[37] with modelling in Coot[38]. The ligand was generated using the ProDRG server[39] then modelled using restraints generated in eLBOW in Phenix[40], and the final structure completed by iterative rounds of model building and refinement in Coot and Phenix. Structure validation was assisted by MolProbity[41] and Phenix. Coordinates and structure factors have been deposited in the Protein Data Bank (www.rcsb.org/pdb) with accession code 6R9W.

Results and Discussion

Structure based virtual screening

The structure based virtual screening workflow employed to identify direct InhA inhibitors is shown in Figure 2. After the top 2,000 compounds, ranked by Glide SP score, were

selected, 81 compounds that showed good Glide SP scores for InhA binding to both InhA-inTyr158 and InhA-outTyr158 conformations were collected. These were subsequently filtered by selection according to Lipinski's rule of five and against PAINS-like properties, yielding 65 compounds (Table S1). The binding affinities of these compounds to both InhA-inTyr158 and InhA-outTyr158 were further evaluated using the more accurate Glide XP mode. These compounds showed Glide XP scores for InhA-inTyr158 and InhA-outTyr158 binding in the ranges 5.1 - 10.2 and 5.6 - 9.3 kcal/mol, respectively. For comparison, the Glide XP scores of two comparator compounds binding to InhA-inTyr158 (2-(*o*-Tolyloxy)-5-hexylphenol (PT70), PDB 2X23) and InhA-outTyr158 (*N*-((3*R*,5*S*)-1-(benzofuran-3-carbonyl)-5-(ethylcarbamoyl)pyrrolidin-3-yl)-3-ethyl-1-methyl-1*H*-pyrazole-5-carboxamide (KV1) PDB 4COD) were -10.5 and -9.1 kcal/mol, respectively. Accordingly, the 16 compounds with the highest Glide XP scores for InhA-inTyr158(< -9.0 kcal/mol) and InhA-outTyr158 (< - 6.9 kcal/mol) were selected for biological evaluation (Table 1). The chemical structures of these compounds are provided (Table S2).

Table 1. Glide XP docking scores and in vitro biological activities of hit compounds.

Compounds	Glide XP docking score (kcal/mol)		Biological activity		
	InhA-inTyr158	InhA-outTyr158	MIC[a] (µg/ml)	Relative inhibition at 1 µM	IC$_{50}$ (µM)
1	-10.9	-7.8	25	66	0.38±0.98
2	-10.6	-7.0	>100	48	NT
3	-10.5	-7.2	>100	23	NT
4	-10.4	-8.3	>100	44	NT
5	-10.3	-7.6	>100	58	NT

|					
6	-10.2	-7.3	>100	4	NT
7	-10.2	-7.1	25	62	0.22±0.97
8	-10.1	-8.0	>100	44	NT
9	-9.9	-7.8	>100	21	NT
10	-9.7	-8.5	>100	45	NT
11	-9.6	-8.2	>100	50	NT
12	-9.4	-7.3	>100	48	NT
13	-9.3	-7.5	>100	57	NT
14	-9.3	-7.7	>100	58	NT
15	-9.2	-6.9	>100	14	NT
16	-9.0	-7.8	>100	35	NT
Triclosan			50	70	0.60±0.94
PT70[b]	-10.5	-	-	-	-
KV1[c]	-	-9.1	-	-	-

[a]MIC value determined against *M. tuberculosis* H37Ra

[b], [c] Reference compounds for Glide XP docking score in InhA-inTyr158 (PDB 2X23) and in InhA-outTyr158 (PDB 4COD), respectively

Anti-tubercular activity

With the lower experimental cost and less administration for biosafety requirement, minimal inhibitory concentration (MIC) values for the 16 hit compounds were evaluated against the avirulent strain of *M. tuberculosis* (H37Ra) (Table 1). Most of these compounds showed no activity against *M. tuberculosis* H37Ra with MIC values more than 100 μg/ml. Importantly, compounds **1** and **7** (Figure 3) showed biological activity, with MIC values of 25 μg/ml.

Accordingly, MIC values for compounds **1** and **7** against the virulent strain of *M. tuberculosis* (H37Rv) were determined. Compound **7** demonstrated equivalent MIC values against both *M. tuberculosis* strains (25 µg/ml), whereas MIC value against *M. tuberculosis* H37Rv of compound **1** is decreased by 2-fold in comparison with that against *M. tuberculosis* H37Ra (12.5 and 25 µg/ml, respectively). Therefore, compounds **1** and **7** screened from our present study are promising lead compounds for the further development of novel anti-tuberculosis agents.
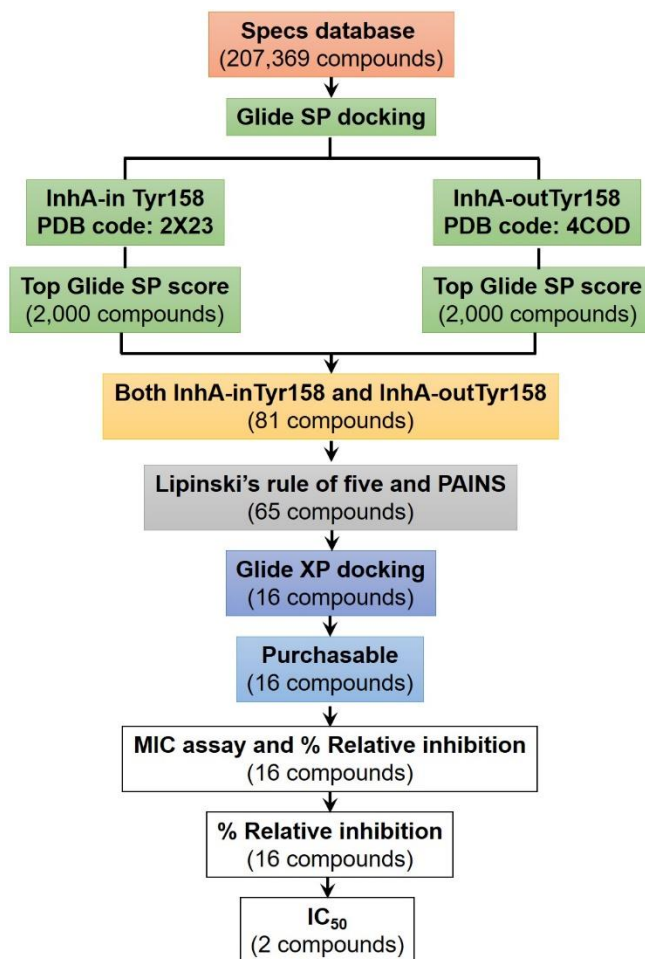

Figure 2. Virtual screening workflow for discovery of direct InhA inhibitors.

compound **1**   compound **7**
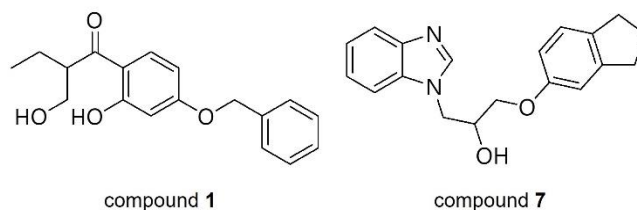
Figure 3. Chemical structures of two active compounds against *M. tuberculosis* (compound **1** and compound **7**).

M. tuberculosis **InhA inhibitory activity**

The activities of the 16 hit compounds were next evaluated in vitro against purified recombinant *M. tuberculosis* InhA. Relative InhA inhibition at a final concentration of 1 µM was evaluated using the known InhA inhibitor triclosan[31] as a reference compound. These experiments gave relative inhibition values for the 16 hit compounds in the range of 4 - 66 %, compared to 70% for triclosan (Table 2). Although all 16 hit compounds displayed lower potency for InhA inhibition than triclosan, the two compounds compound **1** and compound **7** identified as active against *M. tuberculosis* H37Rv both showed relative inhibition values greater than 60%. These data suggest that anti-tubercular activity of these compounds is likely to arise from inhibition of InhA activity. These results motivated determination of IC_{50} values for InhA inhibition by these two compounds, in comparison with triclosan. The results are shown in Figure 4. Compound **1** and compound **7** showed IC_{50} values for InhA inhibition of 0.38 µM and 0.22 µM respectively, compared to a value for triclosan of 0.60 µM (Table 1 and Figure 2). These data demonstrate that both compounds are active in both whole cell and enzyme inhibition assays.
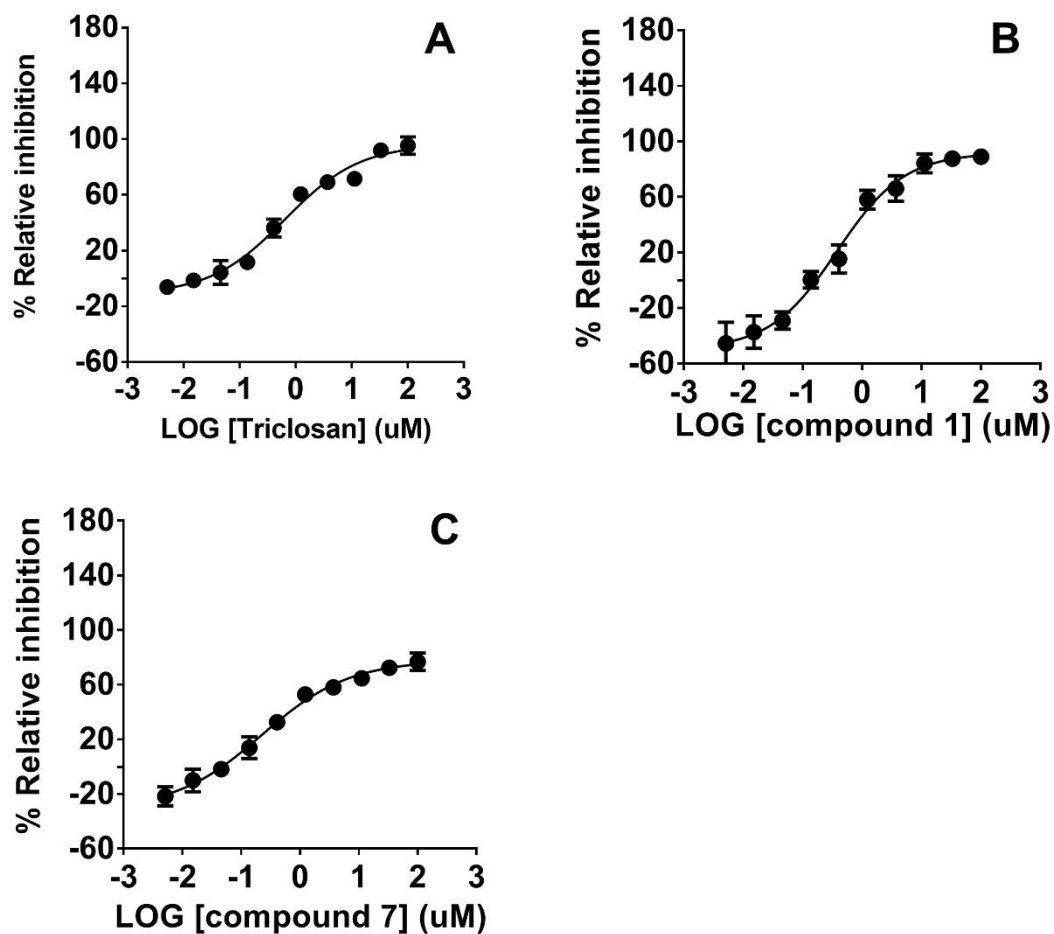
Figure 4. IC_{50} curves fitting for the inhibition of InhA by triclosan (A), compound **1** (B) and compound **7** (C) at various concentrations.

Crystallographic characterization of InhA binding to compound 7

Identification of active compounds motivated investigation of their modes of binding to InhA by X-ray crystallography. Purified recombinant InhA was crystallized in the presence of NADH in the previously reported $C2$ crystal[6] form by hanging-drop vapor diffusion, and crystals exposed to inhibitors before freezing for diffraction data collection. Multiple diffraction experiments on soaked crystals yielded a single dataset (diffracting to a resolution of 1.75 Å (Table 2)) which, after molecular replacement, contained positive difference ($F_o – F_c$) electron density, consistent with the structure of compound **7**, in maps for one of the six InhA molecules present in the crystallographic asymmetric unit. After refinement the real-space correlation

coefficient (RSCC) value (calculated by Phenix)[40] for bound ligand was 0.897, indicating acceptable fit to the experimental electron density.[42] The average B-factor for the bound inhibitor was 31.66 $Å^2$, comparing favorably with a value of 33.64 $Å^2$ for the cofactor (most likely in the NAD^+ form) averaged across the 6 InhA molecules. Binding of compound **7** to the InhA active site is shown in Figure 5.

Compound **7** is bound in the InhA active site in an extended hydrophobic pocket, with the bicyclic indane contacting residues Phe149, Met155, Pro156, Ala157, Ile215 and Leu218; and the benzimidazole ring residues Met103, Ala198, Met199, Ile202 and Leu207. The inhibitor hydroxyl group makes a water-mediated hydrogen bond to the backbone carbonyl of Ala211. Tyr158 is clearly resolved as being in the "in" orientation; other molecules in the asymmetric unit feature Tyr158 in "in" (molecules B and D), "out" (molecules C and F) and dual (molecule E) conformations, indicating that Tyr158 can sample different rotamers in this crystal form. However, our observation of inhibitor bound only to a molecule with Tyr158 in the "in" conformation, coupled with the results of superpositions that indicate a clash between the Tyr158 "out" conformation and the inhibitor indane, strongly support the contention that compound **7** binds preferentially to InhA in the inTyr158 conformation. Surprisingly, the inhibitor binds some distance away from the NAD^+ cofactor, with the closest approach being made by the benzimidazole group to the NAD^+ nicotinamide ring (6.97 Å) and diphosphate (6.58 Å). Interestingly, this mode of binding also differs from those obtained from Glide XP docking of compound **7** against either of the two conformations of InhA (InhA-inTyr158 and InhA-outTyr158). However, there is some partial overlap of the indane binding site with that of the conformation docked against InhA-inTyr158, and between the indane of the conformation docked against InhA-outTyr158 and the crystallographically observed benzimidazole binding site (Figure S1).

InhA has been the subject of extensive efforts aimed at discovery of direct inhibitors, with in consequence numerous crystal structures available for complexes of the enzyme with a range of ligands (for review see Chollet *et al*).[22] We therefore compared our inhibitor-bound structure with those of other InhA complexes, with the aim of identifying the extent to which the observed mode of binding of compound **7** relates to those described for other inhibitors. These comparisons identify the binding mode as most closely resembling that of the C16 substrate

analogue THT (*trans*-2-hexadecenoyl-(*N*-acetylcysteamine)-thioester)) which adopts a U-shaped conformation with the cysteamine/thioester head group contacting the NADH cofactor and the distal end of the aliphatic tail making hydrophobic interactions with multiple residues (Met103, Phe149, Met161, Ala198, Met199, Ala201, Ile202, Leu207, Ile215, and Leu218) of which the majority also participate in compound 7 binding (PDB 1BVR).[3] Of inhibitor complex structures the closest similarity is observed with triclosan binding to its second site (as described in PDB 1P45 in which two triclosan binding sites are observed).[43] However, triclosan and related diaryl ether inhibitors usually bind close to the NAD(H) cofactor, in the binding site utilized by the THT cysteamine group, and this second site is not normally occupied. Importantly, as well as (in common with the majority of InhA complexes) featuring Tyr158 in the "in" conformation, these structures also feature the H6 alpha helix (residues 196 – 206) in an open, but ordered, conformation. This region of the protein adopts a variety of conformations, and is in some cases disordered, in the various InhA structures, and is implicated in substrate binding. These observations lead us to conclude that binding of compound **7** to InhA replicates that of substrate.

Of the multiple other InhA: inhibitor complex structures available the great majority involve inhibitor interactions with cofactor, and the mode of binding observed here is not replicated. There is some partial overlap of compound **7** binding with elements of the binding sites of other inhibitor classes, for example of the indane with the aliphatic tail of the alkylated diaryl ether 8PS (PDB 2B37)[31] , the fluoroenyl group of the aryl carboxamide GENZ10850 (PDB 1P44)[43], or the (4, 4-dimethyl)cyclohexyl group of the 4-hydroxy-2-pyridones NITD-564/916 (PDB 4R9R, 4R9S)[18]; or the benzimidazole with the natural product pyridomycin (chain D of PDB 4BII)[44] or the 2-chloro-6-fluoro-benzyl group of the thiadiazole GSK625 (PDB 5JFO)[16] (Figure S2). However, none of these compounds replicate more than a small fraction of the interactions observed here. Equally, the binding site occupied by compound 7 does not overlap with those of cofactor-independent inhibitors such as the diazaborine AN12855[15] (Figure S2). Taken together, these comparisons indicate that compound **7** adopts an uncommon, substrate-like binding mode that (with the sole exception of the second triclosan site) is not observed in other InhA inhibitors. Similarly, whilst a series of benzimidazole compounds have been reported to inhibit the equivalent enoyl ACP reductase FabI from *Francisella tularensis*, these bind with their benzimidazole moiety close to the cofactor in a binding site distinct from that of compound **7** (Figure S3)[45].

Table 2. Crystallographic data collection and refinement statistics.

Data collection[a]	
Beamline	DLS I03
Space group	*C*2
Molecules/ASU	6
Cell dimensions	
a, *b*, *c* (Å)	100.90, 81.60, 189.42
α, β, γ (°)	90.0, 95.52, 90.0
Wavelength(s) (Å)	0.97624
Resolution (Å)*	43.32 – 1.75 (1.78 – 1.75)
R_{pim}	0.046 (0.389)
$CC_{1/2}$	0.997 (0.765)
$I / \sigma(I)$	10.1 (2.3)
Completeness (%)	99.3 (98.4)
Redundancy	6.9 (6.8)
Refinement	
Resolution (Å)	43.317 – 1.75
No. reflections	152,796
R_{work} / R_{free}	0.1871 / 0.2269
No. non-H atoms	
Protein	11795
Solvent	1031
Inhibitor	23
NAD	264
B-factors	
Protein	39.87
Solvent	38.06
Inhibitor	31.66
NAD	33.64
R.m.s. deviations	
Bond lengths (Å)	0.017
Bond angles (°)	1.480
Ramachandran (%)	
Outliers	0.00

| Favoured | 95.94 |
| PDB code | 6R9W |

[a] Values in parentheses are for highest-resolution shell.
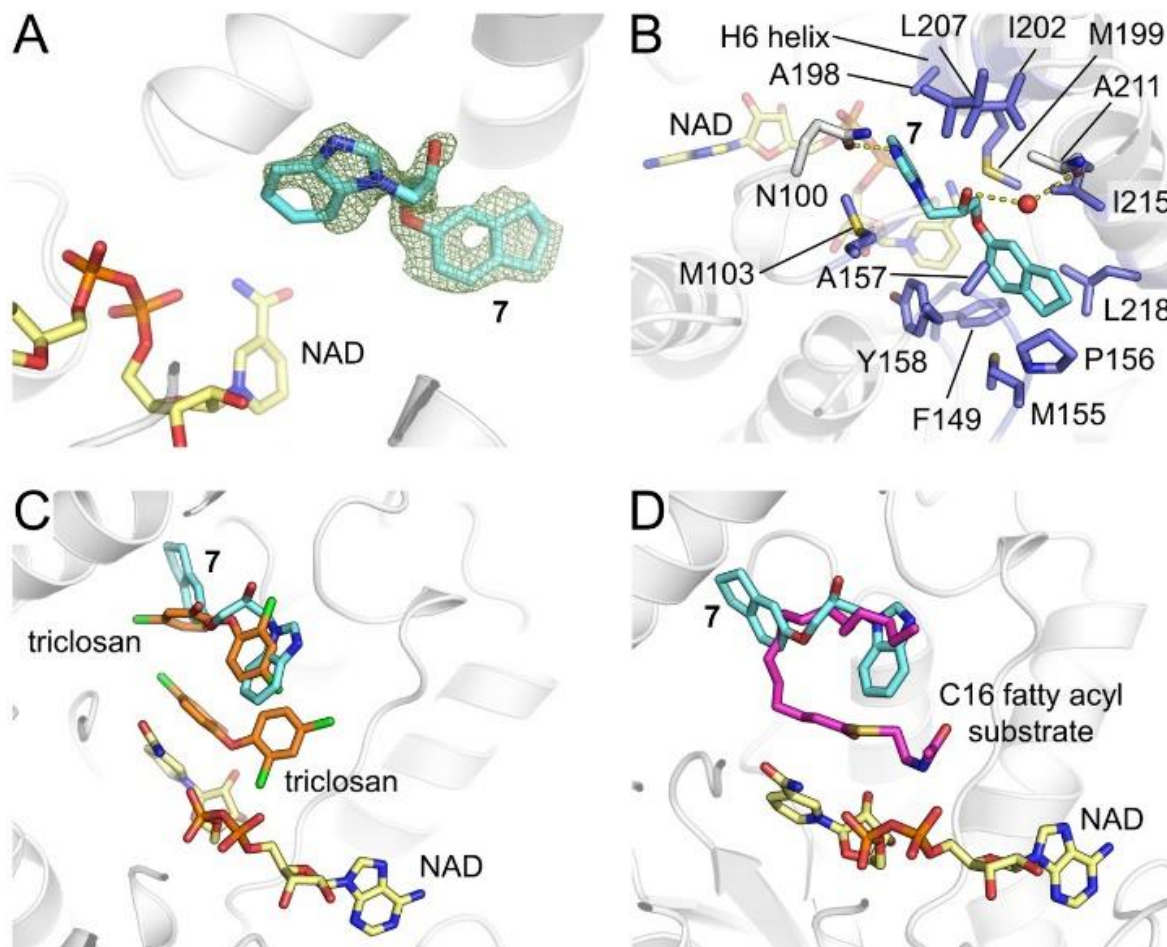
Figure 5. Structure of compound **7** bound to InhA and comparison to other InhA complexes. Compound **7** (cyan sticks) binds in the active site of InhA but does not interact with NAD$^+$ (yellow sticks). (A) compound **7** defined by F_o-F_c electron density (green mesh, contoured at 3σ) calculated after removal of ligand. (B) Binding of compound **7** is stabilised by close interaction with nine hydrophobic residues (labelled, blue sticks). (C) Comparison of compound 7 binding with the two previously determined binding sites for triclosan (PDB 1P45, orange sticks). (D) Comparison of compound **7** binding with a C16 fatty acyl substrate (PDB 1BVR, pink sticks).

Conclusions

The work presented here demonstrates that structure based virtual screening supported by subsequent biological assays can identify novel InhA inhibitors with potential to act as anti-tuberculosis agents. The most active compound, compound **7**, shows encouraging inhibitory activity towards InhA, with an IC_{50} value of 0.22 µM that compares favorably with that of the widely used model compound triclosan (IC_{50} of 0.60 µM). Importantly, this compound also shows activity against *M. tuberculosis* H37Rv in antibacterial assays (MIC of 25 µg/ml) indicating some ability to penetrate mycobacterial cells. A crystal structure of the ternary complex of compound **7** bound to InhA in the presence of cofactor (NAD^+) identifies a mode of binding distinct from that of most other InhA inhibitors, replicating binding of the substrate acyl chain at a site distant from the catalytic center and NAD^+ binding site. These data justify further exploration and optimization of the lead compound as a potential anti-tuberculosis agent.

Supporting Information Available:

Table S1. Glide XP scores of 65 compounds docked into InhA-inTyr158 and InhA-outTyr158

Table S2. Chemical structures of 16 hit compounds

Figure S1. Orientations of compound 7 in the InhA binding site obtained from X-ray crystal structure and Glide XP docking against InhA-inTyr158 and InhA-outTyr158.

Figure S2. Comparisons of the binding site of InhA inhibitors with compound 7. Views from the active site of the InhA:7 crystal structure, with previous structurally characterized inhibitors overlaid to compare their binding modes with 7. For clarity, only the protein backbone and NAD of InhA:7 are shown. (A) GSK-625 (PDB ID 5JFO)16; (B) GSK-SB713 (PDB ID 4QXM)17; (C) NITD-564/916 (PDB IDs 4R9R/4R9S)18; (D) AN12855 (which binds independently of NAD, PDB ID 5VRL).

Figure S3. Comparison of compound 7 binding to InhA with a benimidazole inhibitor of the enoyl ACP reductase (FabI) from Francisella tularensis. The crystal structure of the F. tularensis FabI inhibitor complex (FtuFabI:1, PDB ID 3UIC) is superposed with the InhA:7 structure (RMSD 1.46 Å over 247 Cα). View as in Figure S2.

Acknowledgements

References

(1) World Health Organization (WHO). Global Tuberculosis Report 2018. https://www.who.int/tb/publications/global_report/en/ (accessed June 15, 2018).

(2) World Health Organization (WHO). WHO Treatment Guidelines for Isoniazid-Resistant Tuberculosis: Supplement to the WHO Treatment Guidelines for Drug-resistant Tuberculosis. https://www.who.int/tb/areas-of-work/drug-resistant-tb/MDR_TB_2017.pdf. (accessed June 15, 2018).

(3) Rozwarski, D. Crystal Structure of the *Mycobacterium tuberculosis* Enoyl-ACP Reductase, InhA, In Complex with NAD$^+$ and a C16 Fatty Acyl Substrate. A.; Vilchèze, C.; Sugantino, M.; Bittman, R.; Sacchettini, J.C. *J. Biol. Chem*. **1999**, 274, 15582-15589.

(4) Takayama, K.; Wang, C.; Besra, G. S. Pathway to Synthesis and Processing of Mycolic Acids in *Mycobacterium tuberculosis*. *Clin. Microbiol. Rev*. **2005**, 18, 81-101.

(5)   Banerjee, A.; Dubnau, E.; Quemard, A.; Balasubramanian, V.; Um, K.S.; Wilson, T.; Collins, D.; de Lisle, G.; Jacobs, W. R. Jr. InhA, a Gene Encoding a Target for Isoniazid and Ethionamide in *Mycobacterium tuberculosis*. *Science* **1994**, 263, 227-230.

(6)   Dessen, A.; Quémard, A.; Blanchard, J. S.; Jacobs, W. R. Jr; Sacchettini, J. C. Crystal Structure and Function of the Isoniazid Target of *Mycobacterium tuberculosis*. *Science* **1995**, 267, 1638-1641.

(7)   Quémard, A.; Sacchettini, J. C.; Dessen A, Vilcheze, C.; Bittman, R.; Jacobs, W. R. Jr; Blanchard, J. S. Enzymatic Characterization of the Target for Isoniazid in *Mycobacterium tuberculosis*. *Biochemistry* **1995**, 34, 8235-8241.

(8)   Heym, B.; Alzari, P. M.; Honoré, N.; Cole, S. T. Missense Mutations in the Catalase-Peroxidase Gene, KatG, are Associated with Isoniazid Resistance in *Mycobacterium tuberculosis*. *Mol. Microbiol.* **1995**, 15, 235-245.

(9)   Rouse, D. A.; Li, Z.; Bai, G. H.; Morris, S. L. Characterization of the KatG and InhA Genes of Isoniazid-Resistant Clinical Isolates of *Mycobacterium tuberculosis*. *Antimicrob. Agents Chemother.* **1995**, 39, 2472-2477.

(10)   Blanchard, J. S. Molecular Mechanisms of Drug Resistance in *Mycobacterium tuberculosis*. *Annu. Rev. Biochem.* **1996**, 65, 215-239.

(11)   AlMatar, M.; Makky, E. A.; Var, I.; Kayar, B.; Köksal, F. Novel Compounds Targeting InhA for TB Therapy. *Pharmacol. Rep.* **2018**, 70, 217-226.

(12)   Parikh, S.L.; Xiao, G.; Tonge, P. J. Inhibition of InhA, the Enoyl Reductase from *Mycobacterium tuberculosis*, by Triclosan and Isoniazid. *Biochemistry* **2000**, 39, 7645–7650.

(13)   Holas, O.; Ondrejcek, P.; Dolezal M. *Mycobacterium tuberculosis* Enoyl-Acyl Carrier Protein Reductase Inhibitors as Potential Antituberculotics: Development in the Past Decade. *J. Enzyme Inhib. Med. Chem.* **2015**, 30, 629-648.

(14)   Pan, P.; Tonge, P. J. Targeting InhA, the FASII Enoyl-ACP Reductase: SAR Studies on Novel Inhibitor Scaffolds. *Curr. Top. Med. Chem.* **2012**, 12, 672-693.

(15) Xia, Y.; Zhou, Y.; Carter, D.S.; McNeil, M.B.; Choi, W.; Halladay, J.; Berry, P.W.; Mao, W.; Hernandez, V.; O'Malley, T.; Korkegian, A.; Sunde, B.; Flint, L.; Woolhiser, L.K.; Scherman, M.S.; Gruppo, V.; Hastings, C.; Robertson, G.T.; Ioerger, T.R.; Sacchettini, J.; Tonge, P.J.; Lenaerts, A.J.; Parish, T.; Alley, M. Discovery of A Cofactor-Independent Inhibitor of *Mycobacterium tuberculosis* InhA. *Life Sci. Alliance*. **2018**, 1, e201800025.

(16) Martínez-Hoyos, M.; Perez-Herran, E.; Gulten, G.; Encinas. L.; Álvarez-Gómez, D.; Alvarez, E.; Ferrer-Bazaga, S.; García-Pérez, A.; Ortega, F.; Angulo-Barturen, I.; Rullas-Trincado, J.; Blanco Ruano, D.; Torres, P.; Castañeda, P.; Huss, S.; Fernández Menéndez, R.; González Del Valle, S.; Ballell, L.; Barros, D.; Modha, S.; Dhar, N.; Signorino-Gelo, F.; McKinney, J.D.; García-Bustos, J.F.; Lavandera, J.L.; Sacchettini, J.C.; Jimenez, M.S.; Martín-Casabona, N.; Castro-Pichel, J.; Mendoza-Losana, A. Antitubercular Drugs for An Old Target: GSK693 as a Promising InhA Direct Inhibitor. *EBioMedicine*. **2016**, 8, 291-301.

(17) Guardia, A.; Gulten, G.; Fernandez, R.; Gómez, J.; Wang, F.; Convery, M.; Blanco, D.; Martínez, M.; Pérez-Herrán, E.; Alonso, M.; Ortega, F.; Rullás, J.; Calvo, D.; Mata, L.; Young, R.; Sacchettini, J.C.; Mendoza-Losana, A.; Remuiñán, M.; Ballell Pages, L.; Castro-Pichel, J. *N*-Benzyl-4-((heteroaryl)methyl)benzamides: A New Class of Direct NADH-Dependent 2-*trans* Enoyl-Acyl Carrier Protein Reductase (InhA) Inhibitors with Antitubercular Activity. *ChemMedChem* **2016**, 11, 687-701.

(18) Manjunatha, U.H.; S Rao, S.P.; Kondreddi, R.R.; Noble, C.G.; Camacho, L.R.; Tan, B.H.; Ng, S.H.; Ng, P.S.; Ma, N.L.; Lakshminarayana, S.B.; Herve, M.; Barnes, S.W. Yu, W.; Kuhen, K.; Blasco, F.; Beer, D.; Walker, J.R.; Tonge, P.J.; Glynne, R.; Smith, P.W.; Diagana, T.T. Direct Inhibitors of InhA are Active Against *Mycobacterium tuberculosis*. *Sci. Transl. Med*. **2015**, 7, 269ra3.

(19) Rožman, K.; Sosič, I.; Fernandez, R.; Young, R. J.; Mendoza, A.; Gobec, S.; Encinas, L. A New 'Golden Age' for the Antitubercular Target InhA. *Drug Discovery Today* **2017**, 22, 492-502.

(20) Luckner, S. R.; Liu, N.; am Ende, C. W.; Tonge, P. J.; Kisker, C. A Slow, Tight Binding Inhibitor of InhA, the Enoyl-Acyl Carrier Protein Reductase from *Mycobacterium tuberculosis*. *J. Biol. Chem.* **2010**, 285, 14330-14337.

(21) Encinas, L.; O'Keefe, H.; Neu, M.; Remuiñán, M. J.; Patel, A. M.; Guardia, A.; Davie, C. P.; Pérez-Macías, N.; Yang, H.; Convery, M. A.; Messer, J. A.; Pérez-Herrán, E.; Centrella, P. A.; Alvarez-Gómez, D.; Clark, M. A.; Huss, S.; O'Donovan, G. K.; Ortega-Muro, F.; McDowell, W.; Castañeda, P.; Arico-Muendel, C. C.; Pajk, S.; Rullás, J.; Angulo-Barturen, I.; Alvarez-Ruíz, E.; Mendoza-Losana, A.; Ballell Pages, L.; Castro-Pichel, J.; Evindar ,G. Encoded Library Technology as a Source of Hits for the Discovery and Lead Optimization of a Potent and Selective Class of Bactericidal Direct Inhibitors of *Mycobacterium tuberculosis* InhA. *J. Med. Chem.* **2014**, 57, 1276-1288.

(22) Chollet, A.; Maveyraud, L.; Lherbet, C.; Bernardes-Génisson, V. An Overview on Crystal Structures of InhA Protein: Apo-Form, in Complex with Its Natural Ligands and Inhibitors. *Eur. J. Med. Chem.* **2018**, 146, 318-343.

(23) Parikh, S.; Moynihan, D. P.; Xiao, G.; Tonge, P. J. Roles of Tyrosine 158 and Lysine 165 in the Catalytic Mechanism of InhA, the Enoyl-ACP Reductase from *Mycobacterium tuberculosis*. *Biochemistry* **1999**, 38, 13623–13634.

(24) Shirude, P. S.; Madhavapeddi, P.; Naik, M.; Murugan, K.; Shinde, V.; Nandishaiah, R.; Bhat, J.; Kumar, A.; Hameed, S.; Holdgate, G.; Davies, G.; McMiken, H.; Hegde, N.; Ambady, A.; Venkatraman, J.; Panda, M.; Bandodkar, B.; Sambandamurthy, V. K.; Read, J. A. Methyl-Thiazoles: A Novel Mode of Inhibition with the Potential to Develop Novel Inhibitors Targeting InhA in *Mycobacterium tuberculosis*. *J. Med. Chem.* **2013**, 56, 8533–8542.

(25) Friesner, R. A.; Banks, J. L.; Murphy, R. B., Halgren, T. A., Klicic, J. J.; Mainz, D. T.; Repasky, M. P.; Knoll, E. H.; Shelley, M.; Perry, J. K.; Shaw, D. E.; Francis, P.; Shenkin, P. S. Glide: A New Approach for Rapid, Accurate Docking and Scoring. 1. Method and Assessment of Docking Accuracy. *J. Med. Chem.* **2004**, 47, 1739–1749.

(26) Friesner, R. A.; Murphy, R. B.; Repasky, M. P.; Frye, L. L.; Greenwood, J. R.; Halgren, T. A.; Sanschagrin, P. C.; Mainz, D. T. Extra Precision Glide: Docking and Scoring

Incorporating a Model of Hydrophobic Enclosure for Protein-Ligand Complexes. *J. Med. Chem*. **2006**, 49, 6177–6196.

(27) Halgren, T. A.; Murphy, R. B.; Friesner, R. A.; Beard, H. S.; Frye, L. L.; Pollard, W. T.; Banks, J. L. Glide: A New Approach for Rapid, Accurate Docking and Scoring. 2. Enrichment Factors in Database Screening. *J. Med. Chem*. **2004**, 47, 1750–1759.

(28) Daina, A.; Michielin, O.; Zoete, V. SwissADME: A Free Web Tool to Evaluate Pharmacokinetics, Drug-Likeness and Medicinal Chemistry Friendliness of Small Molecules. *Sci. Rep*. **2017**, 7, 42717.

(29) Lipinski, C. A.; Lombardo, F.; Dominy, B. W.; Feeney, P. J. Experimental and Computational Approaches to Estimate Solubility and Permeability in Drug Discovery and Development Settings. *Adv. Drug Delivery Rev*. **2001**, 46, 3-26.

(30) Baell, J. B.; Holloway, G. A. New Substructure Filters for Removal of Pan Assay Interference Compounds (PAINS) from Screening Libraries and for Their Exclusion in Bioassays. *J. Med. Chem*. **2010**, 53, 2719-2740.

(31) Sullivan, T. J.; Truglio, J. J.; Boyne, M. E.; Novichenok, P.; Zhang, X.; Stratton, C. F.; Li, H. J.; Kaur, T.; Amin, A.; Johnson, F.; Slayden, R. A.; Kisker, C.; Tonge, P. J. High Affinity InhA Inhibitors with Activity Against Drug-Resistant Strains of *Mycobacterium tuberculosis*. *ACS Chem. Biol*. **2006**, 1, 43-53.

(32) Kabsch, W. XDS. *Acta. Crystallogr. D Biol. Crystallogr*. **2010**, 66, 125-132.

(33) Winter, G. Xia2: An Expert System for Macromolecular Crystallography Data Reduction. *J. Appl. Crystallogr.* **2010**, 43, 186-190.

(34) Evans, P. R.; Murshudov, G. N. How Good are my Data and What is the Resolution?. *Acta Crystallogr., Sect. D: Biol. Crystallogr.* **2013**, 69, 1204-1214.

(35) Winn, M. D.; Ballard, C. C.; Cowtan, K. D.; Dodson, E. J.; Emsley, P.; Evans, P. R.; Keegan, R. M.; Krissinel, E. B.; Leslie, A. G.; McCoy, A.; McNicholas, S. J.; Murshudov, G. N.; Pannu, N. S.; Potterton, E. A.; Powell, H. R.; Read, R. J.; Vagin, A.; Wilson, K. S. Overview of the CCP4 Suite and Current Developments. *Acta Crystallogr., Sect. D: Biol. Crystallogr.* **2011**, 67, 235-242.

(36) McCoy, A. J.; Grosse-Kunstleve, R. W.; Adams, P. D.; Winn, M. D.; Storoni, L. C.; Read, R. J. Phaser Crystallographic Software. *J. Appl. Crystallogr*. **2007**, 40, 658-674.

(37) Murshudov, G. N.; Skubák, P.; Lebedev, A. A.; Pannu, N. S.; Steiner, R. A.; Nicholls, R. A.; Winn, M. D.; Long, F.; Vagin, A. A. REFMAC5 for the Refinement of Macromolecular Crystal Structures. *Acta Crystallogr., Sect. D: Biol. Crystallogr.* **2011**, 67, 355-367.

(38) Emsley, P.; Lohkamp, B.; Scott, W. G.; Cowtan, K. Features and Development of Coot. *Acta Crystallogr., Sect. D: Biol. Crystallogr.* **2010**, 66, 486-501.

(39) Schüttelkopf, A. W.; van Aalten, D. M. PRODRG: A Tool for High-Throughput Crystallography of Protein-Ligand Complexes. *Acta Crystallogr., Sect. D: Biol. Crystallogr.* **2004**, 60, 1355-1363.

(40) Adams, P. D.; Afonine, P. V.; Bunkóczi, G.; Chen, V. B.; Davis, I. W.; Echols, N.; Headd, J. J.; Hung, L. W.; Kapral, G. J.; Grosse-Kunstleve, R. W.; McCoy, A. J.; Moriarty, N. W.; Oeffner, R.; Read, R. J.; Richardson, D. C.; Richardson, J. S,; Terwilliger, T. C.; Zwart, P. H. PHENIX: A Comprehensive Python-Based System for Macromolecular Structure Solution. *Acta Crystallogr., Sect. D: Biol. Crystallogr.* **2010**, 66, 213-221.

(41) Chen, V. B.; Arendall, W. B. 3rd; Headd, J. J.; Keedy, D. A.; Immormino, R. M.; Kapral, G. J.; Murray, L. W.; Richardson, J. S.; Richardson, D. C. MolProbity: All-Atom Structure Validation for Macromolecular Crystallography. *Acta Crystallogr., Sect. D: Biol. Crystallogr.* **2010**, 66, 12-21.

(42) Smart, O. S.; Horský, V.; Gore, S.; Svobodová Vařeková, R.; Bendová, V.; Kleywegt, G. J.; Velankar, S. Validation of Ligands in Macromolecular Structures Determined by X-Ray Crystallography. *Acta Crystallogr., Sect. D: Biol. Crystallogr.* **2018**, 74, 228-236.

(43) Kuo, M. R.; Morbidoni, H. R.; Alland, D.; Sneddon, S. F.; Gourlie, B. B.; Staveski, M. M.; Leonard, M.; Gregory, J. S.; Janjigian, A. D.; Yee, C.; Musser, J. M.; Kreiswirth, B.; Iwamoto, H.; Perozzo, R.; Jacobs, W. R. Jr; Sacchettini, J. C.; Fidock, D. A. Targeting Tuberculosis and Malaria Through Inhibition of Enoyl Reductase: Compound Activity and Structural Data. *J. Biol. Chem*. **2003**, 278, 20851-20859.

(44) Hartkoorn, R. C.; Pojer, F.; Read, J. A.; Gingell, H.; Neres, J.; Horlacher, O. P.; Altmann, K. H.; Cole, S. T. Pyridomycin Bridges the NADH- and Substrate-Binding Pockets of the Enoyl Reductase InhA. *Nat. Chem. Biol*. **2014**, 10, 96-98.

(45) Mehboob, S.; Hevener, K.E.; Truong, K.; Boci, T.; Santarsiero, B.D.; Johnson, M.E. Structural and Enzymatic Analyses Reveal the Binding Mode of a Novel Series of *Francisella tularensis* Enoyl Reductase (FabI) Inhibitors. *J. Med. Chem*. **2012**, 55, 5933-5941.

For Table of Contents Only